The DACAPO-PESO campaign: Dynamics, Aerosol, Cloud and Precipitation Observations in the Pristine Environment of the Southern Ocean – an overview

Vogl, T.[1,✉], Schimmel, W.[1], Seifert, P.[2], Kalesse-Los, H.[1], Radenz, M.[2] Ansmann, A.[2], Baars, H.[2], Barja, B.[3], Bühl, J.[2], Engelmann, R.[2], Floutsi, A.[2], Foth, A.[1], Gong, X.[2], Hajipour, M.[2], Henning, S.[2], Jimenez, C.[2], Ohneiser, K.[2], Stratmann, F.[2], Tatzelt, C.[2], Teisseire, A.[2], Wex, H.[2], Witthuhn, J.[1], Zamorano, F.[3]

[1] *University of Leipzig, Leipzig Institute for Meteorology LIM, Leipzig, Germany*
[2] *Leibniz Institute for Tropospheric Research (TROPOS) Leipzig, Germany*
[3] *University of Magallanes, Atmospheric Research Laboratory LIA-UMAG, Punta Arenas, Chile*
✉*e-mail: teresa.vogl@uni-leipzig.de*

Summary: This article gives an overview of the DACAPO-PESO field experiment, which has taken place in Punta Arenas, Chile, from November 2018 to November 2021, and showcases first exciting research results that have already emerged from it.

Zusammenfassung: In diesem Artikel wird ein Überblick über das DACAPO-PESO Experiment gegeben, welches von November 2018 bis November 2021 in Punta Arenas, Chile, stattgefunden hat. Außerdem werden erste spannende Forschungsergebnisse vorgestellt, die bereits daraus gewonnen wurden.

1 Introduction

Punta Arenas, Chile (53°S, 71°W), is located at the southern tip of South America, in the Southern hemispheric mid-latitudinal west wind zone (Fig. 1). With the nearest landmasses (New Zealand) having a distance of roughly 8,000 km towards the direction of the prevailing Westerly winds, the aerosol conditions are dominated by clean Pacific Ocean air masses. Therefore, Punta Arenas as a clean and pristine place in all atmospheric heights is especially well-suited for comparison of atmospheric processes in more aerosol-polluted places in the Northern Hemisphere.
Furthermore, given the general lack of high-quality long-term ground-based remote sensing observations of aerosols and clouds in this region, mainly due to the absence of substantial land masses below 40°S latitude, measurements in the Southern mid-latitudes are extremely useful for better understanding aerosol-cloud-precipitation interactions. For example, the Southern midlatitudes and Sub-Antarctica are a region of large uncertainties in estimates of cloud properties in global climate models, because the supercooled liquid water (SLW) content is underestimated, causing shortwave radiation biases (e.g. Kay et al., 2016). Increasing the SLW content in the models improves these biases, but the reason why parameterizations valid for the Northern Hemisphere are seemingly not

applicable to the Southern Hemisphere is unclear. Aerosol-cloud-interaction and clouds in general still make up the largest uncertainty in climate models (Forster et al., 2021), and it is well known that the number of ice nucleating particles (INPs) varies strongly across Northern and Southern hemispheres (e.g. Gong et al., 2020).

Motivated by the need for an improved process understanding and the current lack of

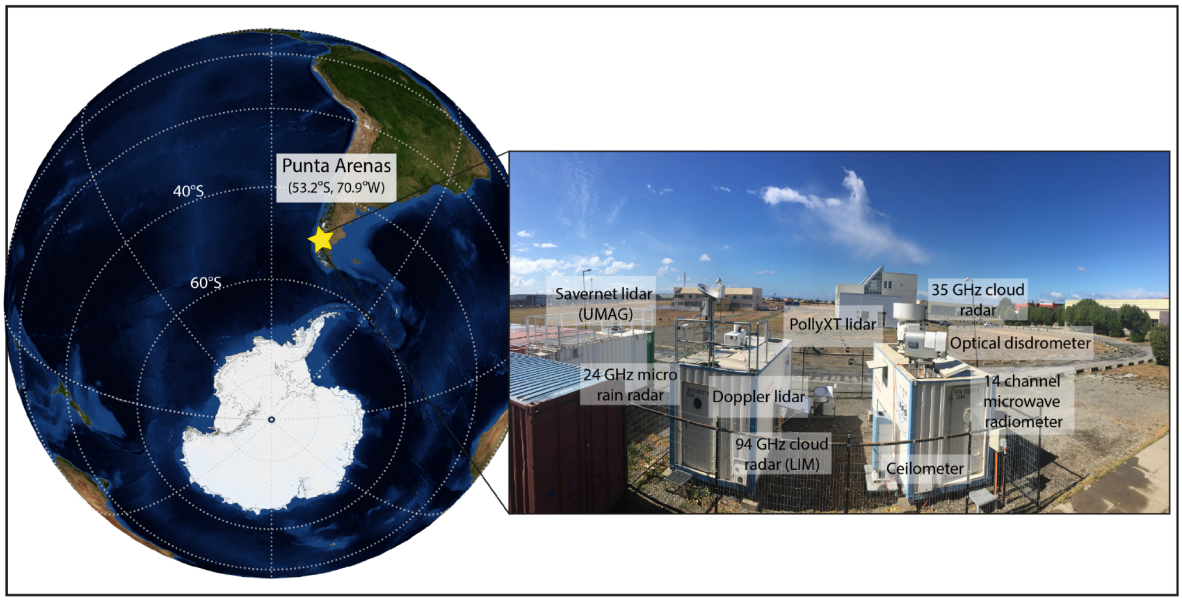

Figure 1: *The location of Punta Arenas on the globe (indicated by a yellow star) in Chile, South America, and the LACROS observational facility, which was enhanced by instruments by the Leipzig Institute for Meteorology (LIM) and the University of Magallanes (UMAG). Figure 1 from Floutsi et al. (2021).*

high-quality continuous aerosol-cloud-precipitation datasets for the Southern Ocean region, the project DACAPO-PESO (Dynamics, Aerosol, Cloud and Precipitation Observations in the Pristine Environment of the Southern Ocean) was realized by Leibniz Institute of Tropospheric Research (TROPOS), Leipzig, Germany and partners from University of Leipzig and University of Magallanes, Punta Arenas, Chile (http://dacapo.tropos.de). In the frame of this project, a large suite of remote sensing and in-situ instruments has been deployed over a period of more than two years in Punta Arenas. This article will give an overview of the field experiment and showcase some research highlights that have already emerged from it.

2 Instrumentation deployed during the DACAPO-PESO field experiment

In the frame of DACAPO-PESO, the Leipzig Aerosol and Cloud Remote Observations System (LACROS) has been operated on the campus of University of Magallanes (53°S, 71°W) in the 3-year period from austral spring of 2018 to austral spring 2021. LACROS comprises a set of state-of-the-art remote-sensing instruments such as a 35-GHz scanning polarimetric cloud radar, multi-wavelength polarization Raman lidars, Doppler lidar, micro rain radar, microwave radiometer, laser disdrometer, as well as sensors for direct and diffuse solar and terrestrial radiation. Until

September 2019, LACROS was enhanced by a 94-GHz Doppler radar of University of Leipzig. A picture of the site can be seen in Fig. 1. In addition, the TROPOS mobile radiation observatory (MORDOR; https://www.tropos.de/en/research/projects-infrastructures-technology/technology-at-tropos/remote-sensing/radiation-measurement-station-bsrn last access: 2022-04-29) performed radiation measurements during the LACROS deployment. The global horizontal irradiance (GHI), diffuse horzontal irradiance (DHI) and direct horizontal irradiance (DNI) were measured with Class A instruments of the type MS-80 (pyranometer) and MS-56 (pyrheliometer), respectively, from the manufacturer EKO Instruments. The measurement uncertainty under clear skies for this class of pyranometers and pyrheliometers was about 2 % (Fountoulakis et al., 2021).
In-situ aerosol instrumentation was installed on the 620-m high peak of Cerror Mirador mountain, 10 km upwind of the LACROS site. At Cerror Mirardor, particle number size distributions in the range from 10 nm to 10 μm were measured using a TROPOS-type mobility particle size spectrometer (MPSS) Wiedensohler et al., 2012 and an aerodynamic particle sizer. Cloud condensation nuclei (CCN) number concentrations at supersaturations (SS) of 0.1 %, 0.2 %, 0.3 %, 0.5 %, and 0.7 % are measured utilizing a CCN counter. In addition, filter samples were collected from 8 May 2019 to 11 March 2020. These filter samples were used for subsequent laboratory measurements of INPs (see Gong et al., 2022 for details).

3 Research highlights

3.1 Evaluation of the Aeolus winds at Punta Arenas using scanning Doppler cloud radar and radio soundings

Aeolus is an Earth Explorer mission of the European Space Agency and aims to measure vertically resolved wind profiles of one wind component (mainly west-east direction) with the goal to improve numerical weather prediction. It is the first European satellite mission having a lidar on-board and the first space mission ever utilizing a HSRL Doppler lidar. Thus, intensive validation efforts are needed – especially in remote places like in Southern South America.
Next to many other instruments, the scanning Doppler cloud radar MIRA-35 was deployed as part of LACROS during DACAPO-PESO. After intensive algorithm development, horizontal winds could be derived from the Velocity-Azimuth-Display (VAD) cloud radar scans performed every 60 minutes in cloudy regions above the measurement site as schematically shown in Fig. 2. These wind products could then be used to validate the *Aeolus* wind products during the two weekly overpasses and delivered valuable input for the algorithm and instrument developers of *Aeolus*. The wind profiles for the overpass indicated in Fig. 2 are shown in Fig. 3. Furthermore, occasional radiosondes have been launched once a week since the beginning of 2020 for the direct evaluation of *Aeolus* winds and to cross-check the radar-derived horizontal winds. From Fig. 3. one can see that a good agreement between the observations is found at the top of the cloud layer and in the local boundary layer showing the great capabilities of Aeolus. For some atmospheric regions in clear sky, for which also no ground-based Doppler observations and no Aeolus Mie winds are available, sporadic offsets of the Aeolus Rayleigh winds in

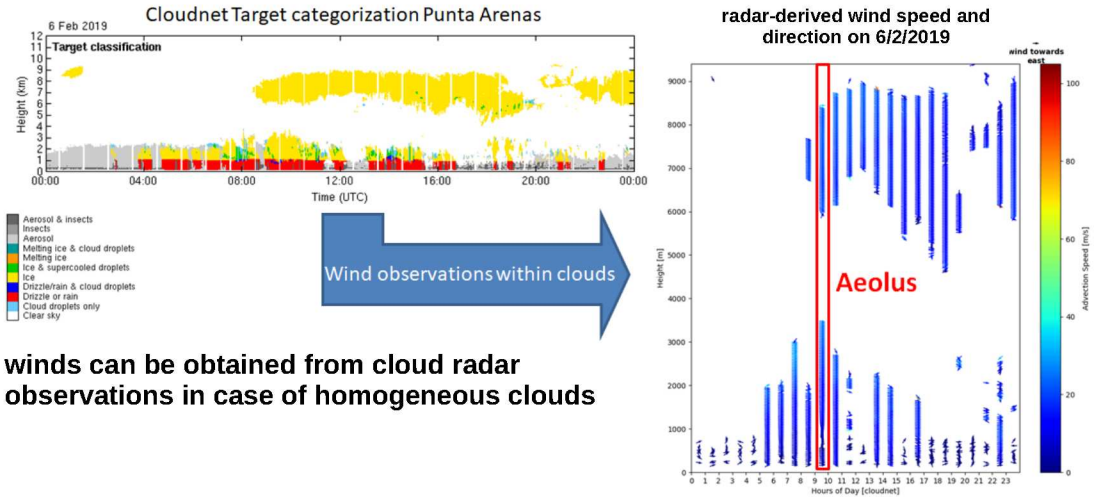

Figure 2: *Sketch for the retrieval of vertical profiles of the horizontal wind vector from scanning Doppler cloud radar. Left, top: Cloudnet Target classification for 6 February 2019. In regions of cloud or precipitation occurrence, e.g. yellow (ice) or red (drizzle), wind speed from radar velocity-azimuth display (VAD) scans can be derived, as shown in the right panel: Cloud radar derived horizontal wind vector for the same day. The overpass time of (satellite) Aeolus is indicated as well.*

comparison to the model data is detected. The reasons for this mismatch are still under investigation.

In general, a good agreement between Aeolus and cloud radar was found, considering the uncertainties of Aeolus and the distance between the two measurement (57 km). Long-term studies have shown that the systematic error is low with the most recent Aeolus algorithms and thus provide proof that space-borne wind profiling is possible and valuable. The radar-derived winds were found to agree very well with the radiosonde winds and thus give confidence for the reliability of this methodology.

3.2 Advection of biomass burning aerosols towards Punta Arenas

During the first 14 months of the DACAPO-PESO campaign, lofted aerosol layers were observed occasionally in the generally clean free troposphere above Punta Arenas. Two events were studied and presented in detail in Floutsi et al. (2021), based on observations from the multiwavelength Raman lidar PollyXT. The lidar observations in combination with a HYSPLIT backward trajectory analysis allowed the identification of the observed aerosol. In the first case (4 and 5 February 2019), the lofted aerosol layers originated from Central and Central-South Chile, and were identified as smoke layers mixed with soil dust, while in the second case (11 March 2019), several geometrically and optically thin smoke layers were observed after long-range transport from Australia. The smoke advection from Central and Central-South Chile affected significantly the available CCN and INP in the lower troposphere. Both CCN and INP concentrations were higher than usual for the first case, and likely contributed to the characteristics of an ice cloud that

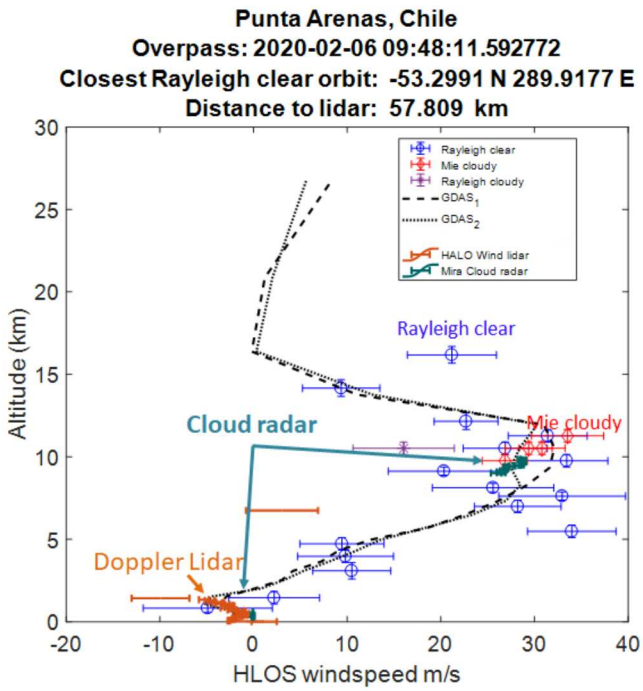

Figure 3: *Comparison of the Aeolus-derived horizontal line-of-sight (HLOS) wind speedto the ones derived from scanning Doppler cloud radar (turquoise) and Doppler lidar(brownish). For Aeolus, wind derived in clear sky regions with the so-called Rayleightechnology (blue) as well as in clouds with the so-called Mie technology (red) andRayleigh one (purple) are shown. For comparison, winds form the Global Data AssimilationSystem (GDAS) are presented, too. A good agreement between the observations is found at the top of the cloud layer and in the local boundary layer showing the great capabilities of Aeolus. For some atmospheric regions in clear sky, for which also no ground-based Doppler observations and no Aeolus Mie winds are available, sporadic offsets of the Aeolus Rayleigh winds in comparison to the model data is detected. The reasons for this mismatch are still under investigation.*

was observed only a couple of hours later. In addition, smoke particles advected from Australia at high altitudes were found to likely facilitate the formation of ice crystals. A long-term analysis of the occurrence of lofted layers was also performed, and, similarly to the ALPACA campaign (i.e. the "Aerosol Lidar Measurement at Punta Arenas in the Frame of Chilean–German Cooperation" which had taken place in Punta Arenas in October 2009, Foth et al., 2019), it was found that lofted aerosol layers in the troposphere were observed more frequently than expected during 2019.

3.3 Australian wildfire smoke in the stratosphere over Punta Arenas during DACAPO-PESO: the decay phase in 2020/21 and impact on ozone depletion

Record-breaking wildfires raged in South-Eastern Australia in late December 2019 and early January 2020 (Ohneiser et al., 2020, 2022). Rather strong pyrocumulonimbus (pyroCb) convection developed over the fire areas and lifted enormous amounts of biomass-burning smoke into the tropopause region. They caused the strongest wildfire-related stratospheric aerosol perturbation ever observed around the globe. The multiwavelength

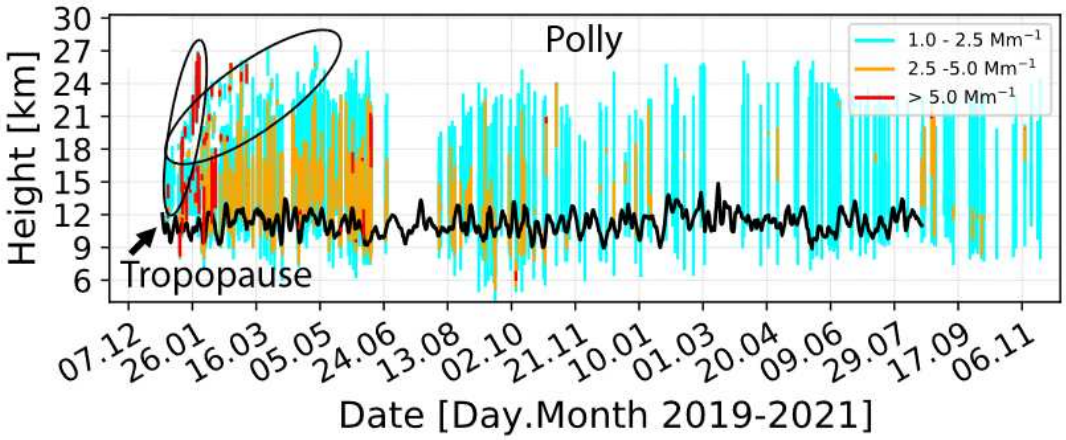

Figure 4: *Overview of Polly XT observations of the UTLS smoke layers (colored bars from layer base to top, one bar per day) from 15 November 2019 to 15 November 2021. Black ellipses indicate the smoke layers showing a fast ascent.*

polarization Raman lidar Polly-XT, which is part of LACROS, was used to monitor this major record-breaking event until the end of 2021. A unique dynamical feature, an anticyclonic, smoke-filled vortex with 1000 km horizontal width and 5 km vertical extent, which ascended by about 500 m per day, was observed over the full last week of January 2020. The key results of the long-term study are as follows: The smoke layers extended, on average, from 9 to 24 km in height. The smoke partly ascended to more than 30 km height as a result of self-lifting processes. Clear signs of a smoke impact on the record-breaking ozone hole over Antarctica in September–November 2020 were found. A slow decay of the stratospheric perturbation detected by means of the 532 nm aerosol optical thickness (AOT) yielded an e-folding decay time of 19–20 months. The maximum upper tropospheric lower stratospheric (UTLS) smoke AOT was around 1.0 over Punta Arenas in January 2020 and thus two to three orders of magnitude above the stratospheric aerosol background of 0.005. After two months with strongly varying smoke conditions, the 532 nm UTLS AOT decreased to 0.03–0.06 from March–December 2020 and to 0.015–0.03 throughout 2021. The particle extinction coefficients were in the range of 10–75 Mm^{-1} in January 2020, and later on mostly between 1 and 5 Mm^{-1} (Fig. 4). Combined lidar-photometer retrievals revealed typical smoke extinction-to-backscatter ratios of 69 ± 19 sr (at 355 nm), 91 ± 17 sr (at 532 nm), and 120 ± 22 sr (at 1064 nm). An ozone reduction of 20–25 % in the 15–22 km height range was observed over Antarctic and New Zealand-based ozonesonde stations in the smoke-polluted air. This smoke-ozone anti-correlation was potentially caused by an enhanced formation of ozone-depleting polar stratospheric clouds on the additional smoke-related particle surface area of 1-5 μm^2 cm^{-3}.

3.4 Ground-based aerosol characterization, including CCN at Cerror Mirardor

In order to gain knowledge on the annual cycle of aerosol particle and CCN number concentrations and the hypothesized seasonality of their sources, long-term in-situ observations at Cerra Mirardor mountain station were carried out. These measurements are also of values for ground truthing the remote sensing observations and retrievals.

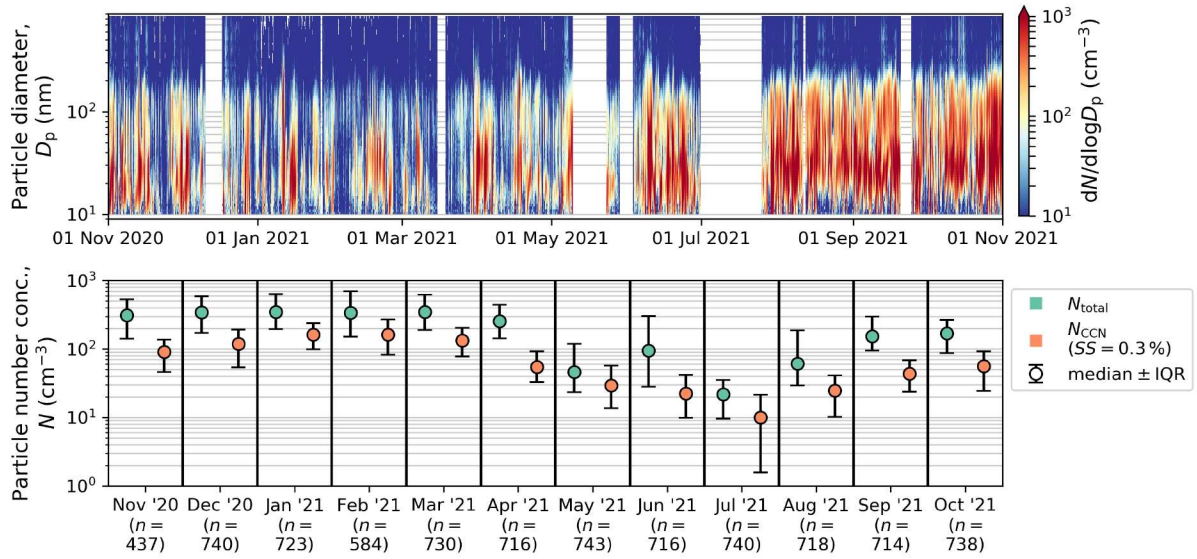

Figure 5: *Top panel: Time series of the particle number size distribution (PNSD) measured at the top of Cerror Mirador between November 2020 and November 2021. Gaps in the PNSD data are due to the instrumentation being unavailable. In the lower panel, monthly averages of the PNSD-derived Ntotal (green) and the CCN number concentration (N_{CCN}) at a 0.3 % SS (orange) are given as median values and their respective inter-quartile ranges (IQR). The number of averaged values, n, is given in the lower panel for reference.*

Particle number size distribution measurements were performed with a combination of a Mobility Particle Size Spectrometer (homebuilt TROPOS) and an Aerodynamic Particle Sizer (APS 3321,TSI, MN, USA) in a particle size range 10 nm to 10000 nm along with the total number concentration (CPC-3772, TSI, MN, USA). The CCN number concentration (CCN-100, DMT, Boulder, USA) was measured at five supersaturation steps.

Atmospheric aerosol particles are important for their radiative effects in the atmosphere, and for their role in the formation of droplets and primary ice in clouds. Total particle number concentrations (N_{total}) were measured at Cerro Mirador with combined measurements from a TROPOS-type MPSS (mobility particle size spectrometer, Wiedensohler et al. (2012), using a concensation particle counter CPC, model 3772, TSI Inc.) and an APS (aerodynamic particle sizer, model 3321, TSI Inc.). CCN were measured using a CCN-counter (model CCN-100, DMT Inc.). More information can be found in Gong et al. (2022). For the measurement period between November 2020 and November 2021, both N_{total} and the CCN number concentration at a SS of 0.3 % ($N_{CCN,\ 0.3}$) covered roughly 2 orders of magnitude when taking the natural variability (indicated by the errorbars in Fig. 5) into consideration. The lowest monthly median values ($N_{total} \approx 20$ cm^{-3} and $N_{CCN,\ 0.3} \approx 10$ cm^{-3}) were found for July 2021, coinciding with the end of the Southern hemispheric winter (May–July). In contrast, concentrations during the summer months (December–February) were roughly one order of magnitude higher ($N_{total} \approx 200$ cm^{-3} and $N_{CCN,\ 0.3} \approx 100$ cm^{-3}).

3.5 A strong continental source of ice-nucleating particles (INPs) at Cerror Mirardor

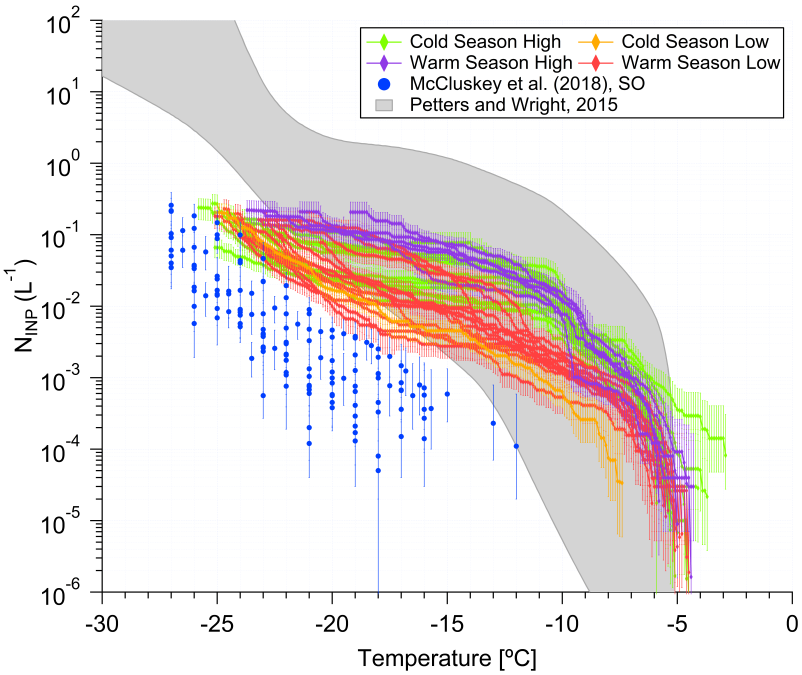

Figure 6: *Spectra of INP concentrations for all examined samples are shown, with the color coding indicating that there were high and low values throughout the year. The gray background shows typical midlatitude continental concentrations, while the blue dots show typical data from the Southern Ocean (SO), free of continental sources.*

INP are important as they are responsible for the formation of primary ice in clouds, and with this they influence cloud radiative processes and the formation or precipitation. To obtain INP concentrations, filter samples were collected at Cerro Mirador, and evaluated off-line at TROPOS, using well proven cold-stages (Gong et al., 2022). At the Cerror Mirardor mountain station, Gong et al. (2022) found unexpectedly high INP number concentrations, comparable to typical continental values, without an annual cycle, but with the typically observed high variability over roughly two orders of magnitude at any freezing temperature (Fig. 6). A large fraction of > 80 % (median value) of all INP was biogenic in nature (for freezing temperatures above -16 °C). An INP parameterization developed for a forest ecosystem (Tobo et al., 2013) was best able to describe the measured data, with 50 % of the predicted INP concentrations within a factor of two of the measured values, but further large deviations of roughly up to plus or minus one order of magnitude. In order to find an explanation for times with high INP concentrations, a range of parameters was investigated, including aerosol parameters and meteorological conditions and air mass back-trajectories. Precipitation was the only parameter which might explain the presence of high INP concentrations because rain drops can disperse bio-aerosol from the soil and from plants into the atmosphere. A comparison with lidar data from the boundary layer showed that particle number concentrations for particles with diameters larger than 500 nm agreed well when continental conditions were assumed in the lidar retrieval. This in turn means that reasonable INP concentrations for the

boundary layer may be obtained based on these lidar data and the above mentioned INP parameterization.

3.6 Hemispheric contrasts in stratiform mixed-phase cloud properties observed with LACROS

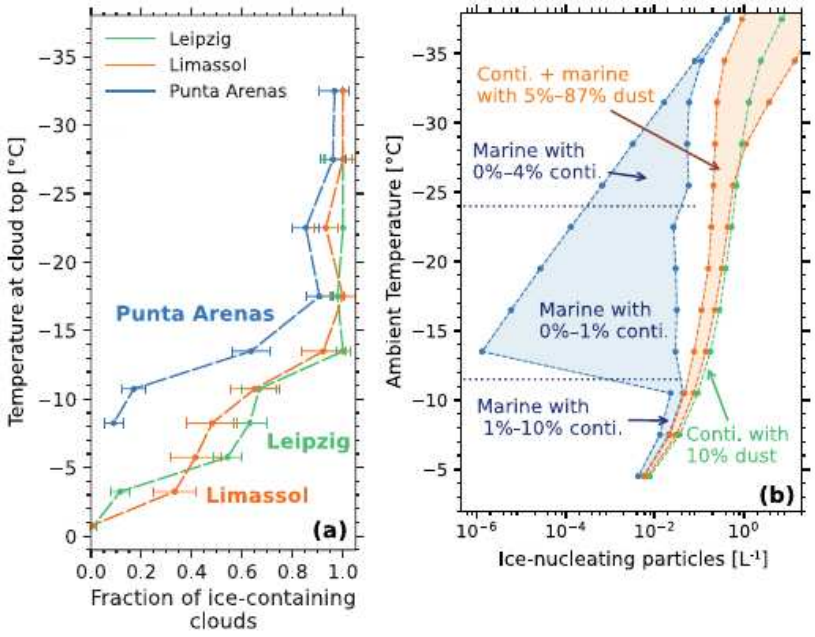

Figure 7: *(a) Fraction of clouds containing ice at a given cloud-top temperature for three different locations: Leipzig (green), Limassol (orange) and Punta Arenas (blue). Only free-tropospheric and turbulent clouds are shown after filtering out gravity wave clouds and boundary layer coupling. (b) Estimated profiles of INP concentrations based on averaged lidar optical data, airmass source and well-established INP parameterizations. At Punta Arenas (blue), the strong increase of INP concentrations for T warmer than -10° C is related to high boundary layer aerosol concentrations.*

The synergistic Cloudnet dataset obtained from the multi-year LACROS observations at Punta Arenas is used to investigate hemispheric contrasts of ice formation in supercooled stratiform clouds. At Punta Arenas, the fraction of ice-containing clouds for a given cloud-top temperature was found to be lower than at two Northern Hemispheric stations (Leipzig, Germany and Limassol, Cyprus) as shown in Fig 7. The low frequency of ice-forming clouds at Punta Arenas at temperatures colder than -15° C can in part be related to orographic gravitiy waves, which create areas of persistent saturation with respect to liquid in the updraft regions. Ice crystals in turn are only observable in the downwind regions. These wave clouds could be identified using the autocorrelation function of the vertical air velocity within the clouds (Radenz et al., 2021). Wave-driven clouds were identified in 30 % of all considered clouds colder than -15° C for the DACAPO-PESO data set. Furthermore, a correlation was found between the surface-coupling of the cloud and the occurrence of ice formation: If a cloud was coupled to the aerosol-laden boundary layer, the probability of ice formation was higher by a fraction of 0.3 to 0.4. Still, even if both gravity wave and boundary layer effects were taken into

account, the probability of ice formation is smaller in clouds over Punta Arenas than for their Northern-hemispheric counterparts (Fig. 7a). This difference is likely related to the lower abundance of INPs in the free troposphere over Punta Arenas.

3.7 Deriving supercooled liquid water beyond lidar attenuation from vertically-pointing cloud radar observations using artificial neural networks

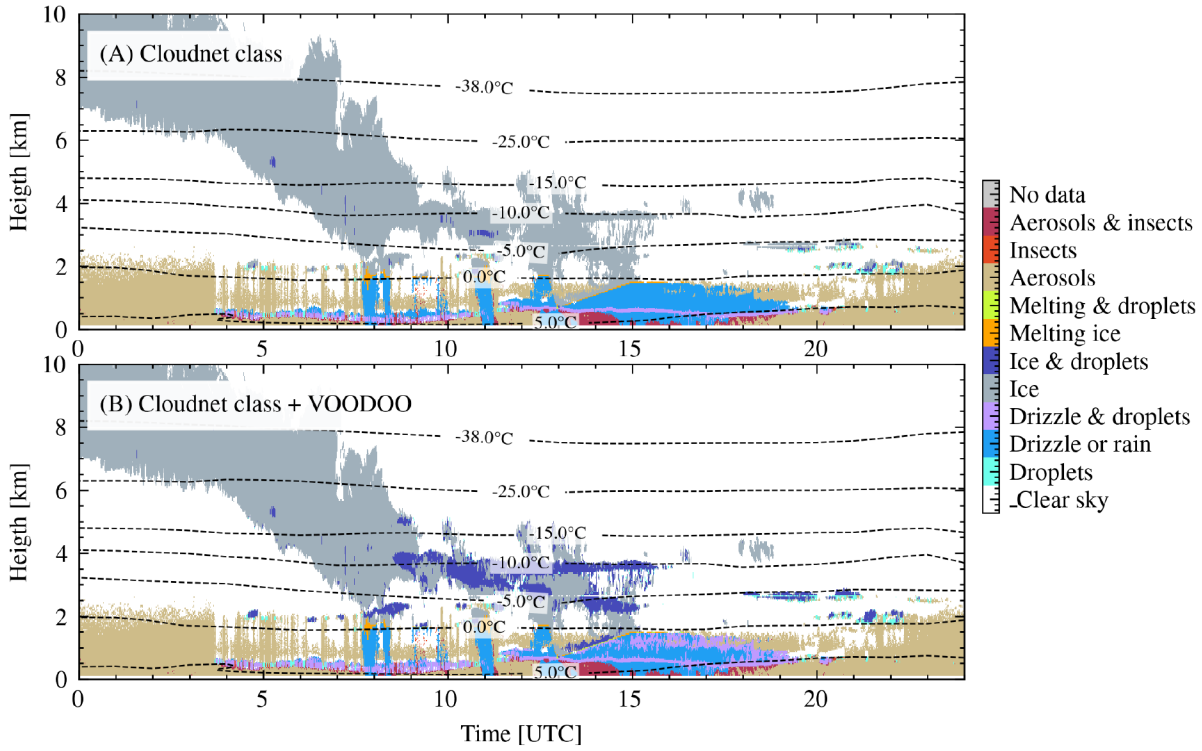

Figure 8: *Example of Cloudnet target classification (top). The lidar was attenuated by the low level liquid cloud at 500 m, (class:Drizzle & rain). VOODOO machine-learning technique (bottom). VOODOO is augmenting the liquid detection of Cloudnet and is able to predict multiple liquid layers between 1 – 4 km altitude (dark blue). Observations were made on 13 March, 2019 in Punta Arenas, Chile.*

The DACAPO-PESO data set was used to develop a novel tool to compute the likelihood for the presence of cloud droplets (CD) using ground-based radar measurements from RPG-FMCW-94-DP Doppler cloud radar, Jenoptik CHM15kx ceilometer, RPG-HATPRO-G2 microwave radiometer and weather model data from the European Centre for Medium-Range Weather Forecasts (ECMWF). Data sets of vertically-pointing Doppler cloud radars and lidars provide insights into cloud properties at high temporal and spatial resolution. However, the identification of liquid CD usually relies on lidar observations, which suffer from complete attenuation at an approximate optical thickness of $\tau > 3$. Since cloud radars can penetrate multiple liquid layers, they can potentially be used to expand the identification of cloud phase to the entire vertical column beyond the lidar signal attenuation height. VOODOO (reVealing supercOOled liquiD beyOnd lidar attenuatiOn) is a deep convolutional neural network (CNN) approach, which uses Doppler radar spectra as input to directly compute the likelihood for the presence of CD at

each data point. VOODOO utilizes concepts of computer vision to relate morphologies in a series of multiple consecutive radar Doppler spectra to the presence of CD. The optimization was done by supervised learning using the Cloudnet target classification (Illingworth et al., 2007) in regions where both radar and lidar signals are available as a-priori ground-truth. Validation was done on suitable case studies as well as long-term observations from two locations, Punta Arenas, Chile (Radenz et al., 2021) and Leipzig, Germany. The PyTorch implementation is freely-available via Zenodo (Schimmel, 2022) and the VOODOO technique is described in detail in Schimmel et al. (2022).

The deep learning approach VOODOO overcomes the issue of droplet underestimation in mixed-phase clouds caused by complete lidar signal attenuation. VOODOO has the potential to drastically improve the hydrometeor phase classification, as displayed in Fig. 8 which shows that VOODOO was able to identify multiple additional mixed-phase layers between 1 and 4 km . The planned fusion of Cloudnet and VOODOO will surely benefit further cloud microphysical and radiative retrievals and thus the cloud remote-sensing community in general.

3.8 Development of a novel machine-learning-based riming retrieval

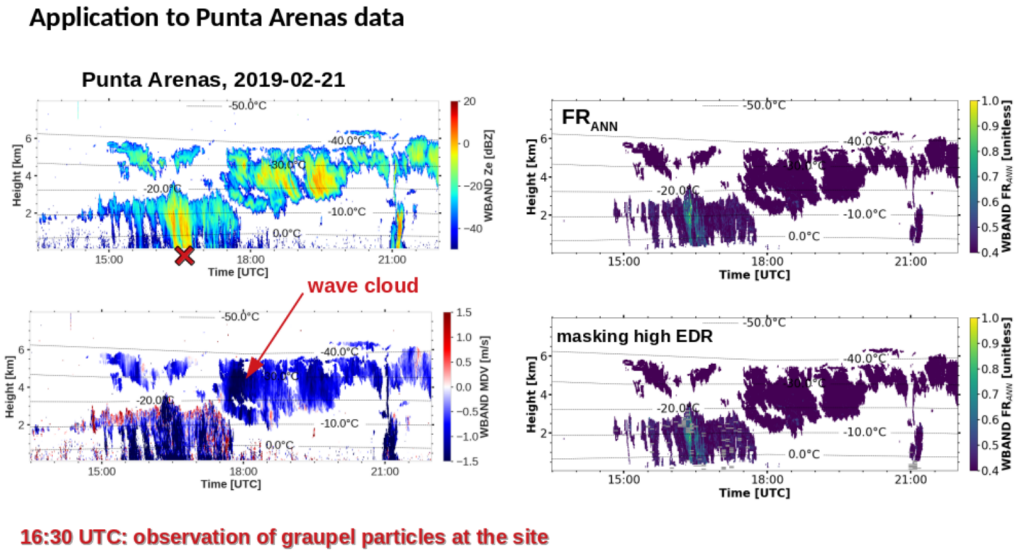

Figure 9: *Radar moments measured by the 94 GHz radar and ANN predictions of riming during a case observed on 21 February 2019: Top left panel shows the equivalent radar reflectivity in dBZ, bottom left panel the mean Doppler velocity. The right-hand panels show the rime fraction FR_{ANN} predicted by the ANN: Top panels shows the raw prediction, and the bottom panel the predictions when pixels with high turbulent eddy dissipation rate (EDR) are masked (grey dashes). The red cross marks the time (16:30 UTC) when graupel particles were observed at the site.*

Riming, i.e. the accretion and freezing of supercooled liquid water (SLW) on ice particles in mixed-phase clouds, is an important pathway for precipitation formation. During this process, droplets of SLW collide with ice hydrometeors and freeze upon contact to the ice surface. This leads to the formation of graupel and hail particles.

Detecting and quantifying riming using ground-based cloud radar observations is of great interest, and the data set acquired during DACAPO-PESO was used to develop and test a method that works even in orographically influenced cloud systems: Artificial neural networks (ANNs) were used to predict riming using ground-based zenith-pointing cloud radar variables as input features. More details on the method can be found in Vogl et al. (2022).
Fig. 9 shows a case study observed on 21 February 2019. A precipitating cloud system with cloud top around 2.5 to 3 km is present from around 15 to 18 UTC. Above, a mid-level cloud with top around 6 km and varying cloud base is observed. At 16:30 UTC, marked by the red cross in Fig. 9, graupel particles were observed at the ground on-site. The predicted rime mass fraction FR_{ANN} maximum is reached around 16:30 UTC, coinciding with the observation of graupel particles. This signal is persistent even if observation points with high turbulent eddy dissipation rate, which masks fingerprints of riming in the cloud radar observations, are excluded.

3.9 Development of a new method to derive the vertical distribution of particle shape

Advancement of the understanding of mixed-phase clouds requires knowledge of microphysical ice growth processes. The transition from pristine to aggregated or rimed particles is a key process in the growth of hydrometeors. A new approach was developed by Teisseire et al. (2022) that uses polarimetric variables from the scanning polarimetric cloud radar MIRA-35, which is part of LACROS, in the 45° slated linear depolarization configuration, to derive the vertical distribution of particle shape (VDPS) between top and base of mixed-phase cloud systems.
The polarimetric parameter SLDR was selected for this study due to its strong sensitivity to shape and low sensitivity to the wobbling effect of particles at different antenna elevation angles. For the VDPS method, elevation scans from 90° to 30° elevation angle were deployed to estimate the vertical profile of the particle shape by means of the polarizability ratio, which is a measure of the density-weighted axis ratio. Results were obtained by retrieving the best fit between observed SLDR-vs-elevation dependencies and respected values simulated with a spheroid scattering model. The applicability of the new method is demonstrated by case studies of isometric, columnar and oblate hydrometeor shapes, which were obtained from measurements during DACAPO-PESO at Punta Arenas. The identified hydrometeor shapes are demonstrated to fit well to the cloud and thermodynamic conditions which prevailed at the times of observations. The VDPS results reveal that the shape gradient ranges in general from a pristine columnar or dendritic state at cloud top toward a more isometric shape at cloud base. Either aggregation or riming processes contribute to this vertical change of microphysical properties. The new height-resolved identification of hydrometeor shape and its gradient is a helpful tool to understand complex processes such as riming or aggregation, which occur particularly in mixed-phase clouds.

4 Summary and conclusions

The DACAPO-PESO data set offers the great opportunity to comprehensibly study aerosol-cloud-precipitation interactions in a unique location in the Southern hemispheric mid-latitudes. As shown, many exciting research results have already been published or are well on the way to be published soon. The following studies were conducted. During DACAPO-PESO, lofted layers of long-range transported smoke were occasionally observed in the clean free troposphere of Punta Arenas. In this study, two events of smoke originating from regional sources in South America and from Australia were captured by the PollyXT lidar and discussed in detail. The in-situ aerosol measurements revealed a strong seasonal cycle (ratio winter/summer 1/10) with in general significantly lower values compared to middle Europe. Continental biological aerosol, the aerosolization of which is most likely driven by raindrops, is the main source of highly ice active INPs in the southernmost Patagonia regions. Regarding contrasts in shallow supercooled clouds, a frequently occurring liquid-only clouds could be attributed to updrafts in gravity waves. When excluding these clouds, a slightly higher frequency of ice-containing clouds in the northern hemisphere can be linked to a higher abundance of ice-nucleating particles. Finally, we show that machine learning techniques can be used to improve current state-of-the-art multi-sensor remote-sensing retrievals in determining the amount and location of mixed-phase cloud volumes and are well suited to retrieve the rime mass fraction form Doppler radar data.

References

Floutsi, A. A., Baars, H., Radenz, M., et al.: Advection of Biomass Burning Aerosols towards the Southern Hemispheric Mid-Latitude Station of Punta Arenas as Observed with Multiwavelength Polarization Raman Lidar, Remote Sens., 13, doi:10.3390/rs13010138, 2021.

Forster, P., Storelvmo, T., Armour, K., et al.: The Earth's energy budget, climate feedbacks and climate sensitivity, in: Climate Change 2021: The Physical Science Basis. Contribution of Working Group I to the Sixth Assessment Report of the Intergouvernmental Panel on Climate Change, edited by Masson-Delmotte, V., Zhwi, P., Pirani, A., et al., Camebridge University Press, 2021.

Foth, A., Kanitz, T., Engelmann, R., et al.: Vertical aerosol distribution in the southern hemispheric midlatitudes as observed with lidar in Punta Arenas, Chile (53.2° S and 70.9° W), during ALPACA, Atmos. Chem. Phys., 19, 6217–6233, doi:10.5194/acp-19-6217-2019, 2019.

Fountoulakis, I., Kosmopoulos, P., Papachristopoulou, K., et al.: Effects of Aerosols and Clouds on the Levels of Surface Solar Radiation and Solar Energy in Cyprus, Remote Sens., 13, doi:10.3390/rs13122319, 2021.

Gong, X., Wex, H., van Pinxteren, M., et al.: Characterization of aerosol particles at Cabo Verde close to sea level and at the cloud level – Part 2: Ice-nucleating particles in air, cloud and seawater, Atmos. Chem. Phys., 20, 1451–1468, doi:10.5194/acp-20-1451-2020, 2020.

Gong, X., Radenz, M., Wex, H., et al.: Significant continental source of ice-nucleating particles at the tip of Chile's southernmost Patagonia region, Atmos. Chem. Phys. Discuss., 2022, 1–29, doi:10.5194/acp-2022-71, 2022.

Illingworth, A. J., Hogan, R. J., O'Connor, E., et al.: Cloudnet: Continuous Evaluation of Cloud Profiles in Seven Operational Models Using Ground-Based Observations, B. Am. Meteorol. Soc., 88, 883–898, doi:10.1175/BAMS-88-6-883, 2007.

Kay, J. E., Bourdages, L., Miller, N. B., et al.: Evaluating and improving cloud phase in the Community Atmosphere Model version 5 using spaceborne lidar observations, J. Geophys. Res. Atmos., 121, 4162–4176, doi:10.1002/2015jd024699, 2016.

Ohneiser, K., Ansmann, A., Baars, H., et al.: Smoke of extreme Australian bushfires observed in the

stratosphere over Punta Arenas, Chile, in January 2020: optical thickness, lidar ratios, and depolarization ratios at 355 and 532 nm, Atmos. Chem. Phys., 20, 8003–8015, doi:10.5194/acp-20-8003-2020, 2020.

Ohneiser, K., Ansmann, A., Kaifler, B., et al.: Australian wildfire smoke in the stratosphere: the decay phase in 2020/21 and impact on ozone depletion, Atmos. Chem. Phys. Discuss., 2022, 1–41, doi:10.5194/acp-2021-1097, 2022.

Radenz, M., Bühl, J., Seifert, P., et al.: Hemispheric contrasts in ice formation in stratiform mixed-phase clouds: Disentangling the role of aerosol and dynamics with ground-based remote sensing, Atmospheric Chemistry and Physics Discussions, 2021, 1–34, doi:10.5194/acp-2021-360, 2021.

Schimmel, W.: pyLARDA3 v0.1, doi:10.5281/zenodo.5970206, 2022.

Schimmel, W., Kalesse-Los, H., Maahn, M., et al.: Identifying cloud droplets beyond lidar attenuation from vertically-pointing cloud radar observations using artificial neural networks, Atmos. Meas. Tech. Discuss., 2022, 1–35, doi:10.5194/amt-2022-149, 2022.

Teisseire, A., Seifert, P., Bühl, J., and Radenz, M.: Determination of the vertical distribution of in-cloud particle shape using SLDR-mode 35-GHz scanning cloud radar, in prep. for Atmos. Meas. Tech. Discuss., 2022.

Tobo, Y., Prenni, A. J., DeMott, P. J., et al.: Biological aerosol particles as a key determinant of ice nuclei populations in a forest ecosystem, J. Geophys. Res. Atmos., 118, 10,100–10,110, doi:https://doi.org/10.1002/jgrd.50801, 2013.

Vogl, T., Maahn, M., Kneifel, S., et al.: Using artificial neural networks to predict riming from Doppler cloud radar observations, Atmos. Meas. Tech., 15, 365–381, doi:10.5194/amt-15-365-2022, 2022.

Wiedensohler, A., Birmili, W., Nowak, A., et al.: Mobility particle size spectrometers: harmonization of technical standards and data structure to facilitate high quality long-term observations of atmospheric particle number size distributions, Atmos. Meas. Tech., 5, 657–685, doi:10.5194/amt-5-657-2012, 2012.